Polyamine pathway contributes to the pathogenesis of Parkinson disease

Nicole M. Lewandowski[a,b], Shulin Ju[c], Miguel Verbitsky[a,d], Barbara Ross[a], Melissa L. Geddie[e], Edward Rockenstein[f,g], Anthony Adame[f], Alim Muhammad[a], Jean Paul Vonsattel[a,h], Dagmar Ringe[c], Lucien Cote[a,i], Susan Lindquist[e], Eliezer Masliah[f,g], Gregory A. Petsko[c,1], Karen Marder[a,i,j], Lorraine N. Clark[a,d,h], and Scott A. Small[a,i,1]

[a]Taub Institute for Research on Alzheimer's Disease and the Aging Brain, [d]Center for Human Genetics, and Departments of [b]Cellular, Molecular, and Biophysical Studies, [i]Neurology, [h]Pathology, and [j]Psychiatry, Columbia University College of Physicians and Surgeons, New York, NY 10032; [c]Departments of Biochemistry and Chemistry and Rosenstiel Basic Medical Sciences Research Center, Brandeis University, Waltham, MA 02454; [e]Whitehead Institute for Biomedical Research and Howard Hughes Medical Institute, Department of Biology, Massachusetts Institute of Technology, Cambridge, MA 02142; and Departments of [f]Neurosciences and [g]Pathology, University of California at San Diego, La Jolla, CA 92093

Contributed by Gregory A. Petsko, August 16, 2010 (sent for review March 31, 2010)

The full complement of molecular pathways contributing to the pathogenesis of Parkinson disease (PD) remains unknown. Here we address this issue by taking a broad approach, beginning by using functional MRI to identify brainstem regions differentially affected and resistant to the disease. Relying on these imaging findings, we then profiled gene expression levels from postmortem brainstem regions, identifying a disease-related decrease in the expression of the catabolic polyamine enzyme spermidine/spermine N1-acetyltransferase 1 (SAT1). Next, a range of studies were completed to support the pathogenicity of this finding. First, to test for a causal link between polyamines and α-synuclein toxicity, we investigated a yeast model expressing α-synuclein. Polyamines were found to enhance the toxicity of α-synuclein, and an unbiased genome-wide screen for modifiers of α-synuclein toxicity identified Tpo4, a member of a family of proteins responsible for polyamine transport. Second, to test for a causal link between SAT1 activity and PD histopathology, we investigated a mouse model expressing α-synuclein. DENSPM (N1, N11-diethylnorspermine), a polyamine analog that increases SAT1 activity, was found to reduce PD histopathology, whereas Berenil (diminazene aceturate), a pharmacological agent that reduces SAT1 activity, worsened the histopathology. Third, to test for a genetic link, we sequenced the SAT1 gene and a rare but unique disease-associated variant was identified. Taken together, the findings from human patients, yeast, and a mouse model implicate the polyamine pathway in PD pathogenesis.

functional MRI | SAT1 | brainstem

Parkinson disease (PD) is the second most common neurodegenerative disease. Although many of the pathogenic molecules underlying the rare autosomal-dominant forms of PD have been identified (1), the full complement of pathogenic pathways involved in the common "sporadic" form of PD remains unknown (2). In principle, gene expression-profiling techniques such as microarray are well suited to identify molecular pathways contributing to the pathogenesis of complex diseases (3). In practice, however, microarray applied to diseases of the brain present a number of analytic challenges (4). Pinpointing regions within the same brain structure that are differentially targeted by and resistant to a disease can be used to address these challenges (4). Specifically, a 2 × 2 factorial ANOVA can be designed, including both within- and between-group factors, and this "double subtraction" is effective in improving signal-to-noise in a microarray experiment (5).

Although the basal ganglia have been clearly implicated in PD, we decided to focus on the brainstem. Postmortem studies mapping α-synuclein inclusions have suggested that brainstem nuclei, in particular the dorsal motor nucleus of the vagus (DMNV), might be affected early in the course of the disease (6). Notably, α-synuclein inclusions in the brainstem are associated with relatively less gliosis and cell death compared with the basal ganglia. Because gliosis and cell death affect expression profiles independent of pathogenic mechanisms, they act to confound the interpretation of gene expression studies.

Nevertheless, the lack of gliosis and cell death raises the question whether α-synuclein inclusions in the brainstem are functionally benign. Though it is true that early nonmotor PD symptoms might implicate the DMNV (7, 8), these clinical observations are only circumstantial. Accordingly, our first goal was to use a high-resolution variant of functional MRI (fMRI) that maps basal cerebral blood volume (CBV) with submillimeter resolution (9, 10) to show that the DMNV is dysfunctional in PD. Furthermore, brainstem fMRI identified the inferior olivary nucleus (ION) as a neighboring region relatively unaffected. Guided by these imaging findings, we generated gene expression profiles of the DMNV and ION harvested from postmortem brains with and without PD. A 2 × 2 factorial analysis, using ION expression levels as a within-brain control, identified a handful of molecules whose expression levels were differentially affected in the DMNV of PD cases.

Establishing whether a molecular pathway isolated by microarray is indeed pathogenic is difficult and requires additional studies (4). At the very least, studies in cell and animal models must show that manipulating the molecular pathway affects measures of the disease, or more ambitiously, genetic studies might identify disease-associated variants in genes involved in the pathway. Among the findings that emerged from our microarray analysis, we decided to dedicate further investigating into an observed decrease in the expression of spermidine/spermine N1-acetyltransferase 1 (SAT1). SAT1 is the rate-limiting catabolic enzyme in the polyamine metabolic pathway (11), and a decrease in SAT1 expression results in increased levels of higher-order polyamines, spermine and spermidine. Notably, previous studies have suggested that polyamines increase α-synuclein aggregation (12, 13) in in vitro systems. Accordingly, we completed a wide range of additional studies using yeast models, mouse models, and human genetics to address separate but complementary questions about the pathogenicity of the polyamine pathway in PD.

Results

High-Resolution fMRI Identifies Brainstem Regions Targeted by and Resistant to PD. To determine whether the DMNV is dysfunctional in PD, CBV maps of the brainstem were generated with fMRI in five PD patients (mean age = 56.4 y) and five healthy age matched controls (mean age = 56.2 y). For each individual subject, ana-

Author contributions: D.R., S.L., E.M., G.A.P., L.N.C., and S.A.S. designed research; N.M.L., S.J., M.V., B.R., M.L.G., E.R., A.A., A.M., and L.N.C. performed research; J.P.V., L.C., and K.M. contributed new reagents/analytic tools; S.A.S. analyzed data; and N.M.L., G.A.P., K.M., L.N.C., and S.A.S. wrote the paper.

The authors declare no conflict of interest.

Freely available online through the PNAS open access option.

Data deposition: The microarray data reported in this paper have been deposited in the Gene Expression Omnibus (GEO) database, www.ncbi.nlm.nih.gov/geo (accession no. GSE19587).

[1]To whom correspondence may be addressed. E-mail: sas68@columbia.edu or petsko@brandeis.edu.

This article contains supporting information online at www.pnas.org/lookup/suppl/doi:10.1073/pnas.1011751107/-/DCSupplemental.

tomical criteria were used to identify a single slice that contained the DMNV (Fig. 1*A* and *SI Text*).

CBV maps of the brainstem slice that contained the DMNV were spatially coregistered, and an unbiased pixel-based analysis revealed a selective disease associated CBV decrease in the general locale of the DMNV (Fig. 1*B*), whereas other areas of the medulla showed no difference between controls and PD patients, including the ION (Fig. 1*B*). To further confirm this finding, three ROIs were generated over the dorsal medulla, with the central ROI overlying the DMNV (Fig. 1*C*). A repeated-measures ANOVA revealed a significant group by region interaction ($F = 7.0$; $P = 0.011$) driven by a selective disease-associated CBV decrease in the central ROI overlying the DMNV (Fig. 1*D Left*). An ROI analysis of the ION further confirmed that this nucleus is relatively resistant to PD (Fig. 1*D Right*).

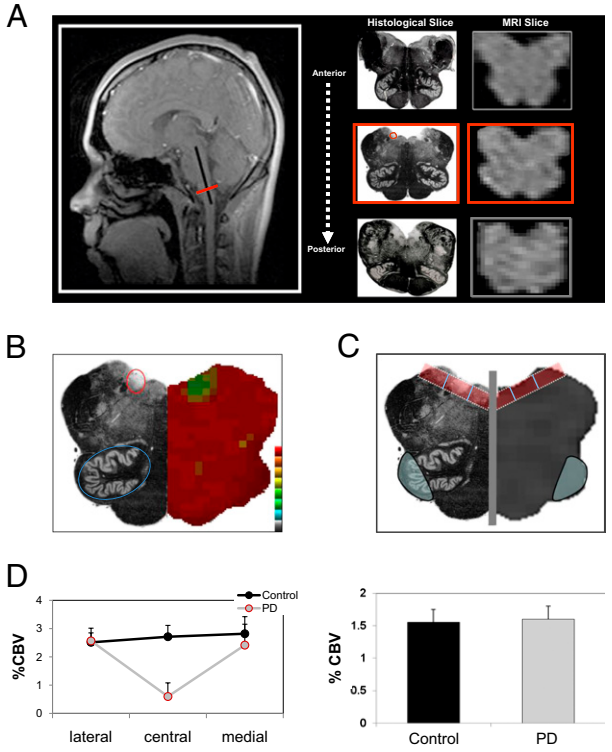

Fig. 1. fMRI identifies brainstem regions targeted by and resistant to PD. (*A*) Anatomical criteria used to identify an MRI slice of the medulla that contains the DMNV. As shown by the sagittal scout image (*Left*), MRI slices were acquired from anterior to posterior (three consecutive MRI slices are shown together with their accompanying histological slices), perpendicular to the long axis of the brainstem (black line in scout image). Using strict anatomical criteria (*Materials and Methods* and *SI Text*), a single slice (red line in scout image and red-boxed middle images) was identified in each individual subject, containing the DMNV (red circle in the middle boxed histological slice). (*B*) CBV fMRI maps of the brainstem slice that contains the DMNV were coregistered, and statistical maps comparing PD patients and controls were generated. For anatomical reference, the right half of the figure shows the statistical maps, which are color-coded such that cooler colors indicate less function, and the left half of the figure shows a histological slice where the DMNV is circled in red and the ION is circled in blue. (*C*) ROI analysis of the DMNV and the ION. The gray vertical line demarcates the midline of the medulla. The red boxes represent the three ROIs in the dorsal medulla, where the box furthest from the midline is the lateral measure, the box closest to the midline represents the medial measure, and the middle box represents the central measure, which contains the DMNV. The blue ovals represent the ROI of the ION. Again, as an anatomical reference, the right half of the figure is the MRI scan, and the left half of the figure is the histological slice. (*D*) Group data analysis shows selective PD-related dysfunction in the central dorsal medulla (*Left*). The *y* axis = %CBV for each ROI (lateral, central, and medial), averaged for PD cases and controls, of both the left and right side of the medulla. No group differences were observed in the ION (*Right*).

Imaging-Guided Microarray Identifies a PD-Associated Decrease in SAT1 Expression. Relying on these imaging findings, we harvested the DMNV and the ION from six postmortem brains with evidence of PD and five control brains. The postmortem PD cases were evaluated for pathological changes (Lewy body-containing neurons and Lewy neurites evidenced with antibodies directed against α-synuclein aggregates) that matched the pattern proposed by Braak (6). Further neuropathological evaluation was performed to confirm the diagnosis of PD over related diseases (*SI Text*), and the DMNV in all cases was positive for α-synuclein aggregates. Microarray techniques were used to generate gene expression profiles for each of the 22 tissue samples.

A repeated-measures 2 × 2 factorial ANOVA model constructed for the imaging study was applied to the expression dataset, in which expression levels from two regions of the medulla (DMNV vs. ION) were included as the within-group factor, diagnosis (PD vs. Control) was the between group factor, and age and sex were included as covariates. Results revealed 10 transcripts whose expression levels showed a significant diagnosis by region interaction below a *P* value of 0.005. These 10 transcripts were all down-regulated in PD vs. Control (Fig. 2*A*).

Informed by previous studies (12, 13), we decided that among the transcripts that emerged from our microarray study, further investigation was warranted for spermidine/spermine N1-acetyltransferase 1 (SAT1), an enzyme that catalyzes the acetylation of polyamines spermidine and spermine. Because decreases in mRNA do not always indicate a decrease in protein levels (14), we harvested the DMNV and ION from a new set of postmortem PD and control brains, and measured both SAT1 and Actin by Western blot analysis. Replicating and extending the microarray finding (Fig. 2*B Left*), results revealed a PD-specific decrease in SAT1 protein, normalized to Actin, in DMNV ($P = 0.045$) but not in the ION ($P = 0.19$; Fig. 2*B Center* and *Right*). Because α-synuclein inclusions are found predominately in neurons, we used immunohistochemistry to show that SAT1 is expressed in neurons of both the DMNV and the ION (Fig. 2*C*).

Yeast Studies Establish a Link Between Polyamines and α-Synuclein. A decrease in SAT1 increases levels of higher-order polyamines (spermidine and spermine). Previous in vitro studies have suggested that polyamines increase the aggregation of α-synuclein (12, 15, 16). To investigate the relationship between polyamines and α-synuclein in an in vivo system, we turned to an established yeast model of α-synuclein toxicity (17). In this model, yeast expressing one copy of α-synuclein grow normally (NoTox strain), cells expressing ∼40% higher levels grow slowly (IntTox), and cells expressing twice as much protein die (HiTox), recapitulating the extreme dosage sensitivity this protein displays in association with PD in humans (18).

We examined the effects of exogenous spermine on yeast strains expressing either wild-type α-synuclein (Syn-WT) or the A53T α-synuclein mutant (Syn-A53T). This mutation enhances the toxicity of α-synuclein both in vitro (19) and in yeast (17), and is associated with the autosomal-dominant form of familial Parkinson's disease in man (20). Spermine was found to be more toxic to yeast expressing α-synuclein (wild-type and A53T) than the strain carrying the empty vector (Fig. 3*A*), suggesting a relationship between polyamines and the cellular toxicity of α-synuclein.

IntTox, the strain with intermediate levels of α-synuclein expression, provides a sensitized background for detecting genes that enhance or suppress toxicity. When α-synuclein accumulates to toxic levels in this strain, one of the earliest detectable defects is a block in the trafficking of secretory vesicles from the endoplasmic reticulum to the Golgi. Proteins that promote forward-vesicle trafficking (e.g., the Rab1 GTPase, Ypt1) suppress α-synuclein toxicity, whereas those that inhibit it (e.g., the Rab1 GTPase activating protein, Gyp8) enhance it (16). In an unbiased genome-wide screen for modifiers of α-synuclein toxicity, we recovered Tpo4 as an enhancer of toxicity (21). Tpo4 is a member of a family of proteins responsible for polyamine transport in *Saccharomyces cerevisiae* (22). Quantitative tests of Tpo4, relative to Ypt1 and Gyp8, confirmed the effect of this polyamine transporter in enhancing the toxicity of α-synuclein when overexpressed (Fig. 3*B*).

A

	Genbank Acc.#	Control Levels		PD Levels		P value
		DMNV	ION	DMNV	ION	
Integrin, beta 1	BG500301	3873	2735	2131	3248	0.0014
Glycoprotein M6B	N63576	4656	3240	3535	6012	0.0021
Spermidine Spermine N1-acetyltransferase	M55580.1	2857	1840	1518	2504	0.0022
Ribosomal protein L36a	NM_001001.1	1124	1056	828	1352	0.0025
DEADH (AspGluAlaAspHis) box polypeptide 17	Z97056	6169	4089	4518	7170	0.0027
Hypothetical protein FLJ10154	NM_018011.1	896	798	844	1309	0.0028
Heterogeneous nuclear ribonucleoprotein A1	AL568186	11566	7281	5733	10631	0.0041
Lactate dehydrogenase B	BE042354	7789	5306	4960	7996	0.0043
Syndecan binding protein (syntenin)	NM_005625.1	2959	1683	1801	3057	0.0044
Similar to splicing factor arginine/serine-rich 2	BC006181.1	1892	1687	1667	2473	0.0048

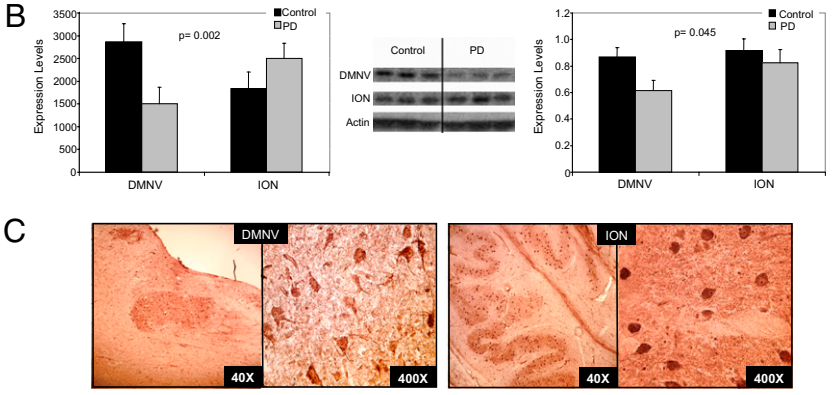

Fig. 2. Imaging-guided microarray identifies a PD-associated decrease in SAT1 expression. (*A*) Ten molecules whose expression levels via microarray analysis were differentially affected in PD cases vs. controls, comparing the DMNV to the ION. Note that for all 10 transcripts, the expression level was down-regulated in PD vs. controls; *P* values were calculated by a repeated-measures 2 × 2 factorial ANOVA. (*B*) Mean expression levels are shown on the graph for SAT1 for mRNA where $n = 22$ (six DMNV and six ION for PD, and five for each region in controls). Expression within the DMNV was significantly down in PD compared with controls ($P = 0.002$) (*Left*). In a new set of brains, protein expression via Western blot, where $n = 20$ (five DMNV and five ION for each group, control and PD), showed a significant decrease of SAT1 expression ($P = 0.045$) in the DMNV of PD samples compared with controls, but not in the ION, as seen in the blot image of representative samples and quantified normalized to actin depicted in the right graph. (*C*) Immunohistochemistry for SAT1 protein in the DMNV (*Left*) and the ION (*Right*) showed positive expression within the neuronal cell bodies of both regions, at 40× (*Left*) and 400× (*Right*), respectively.

Notably, in the IntTox strain, overexpression of Tpo4 caused α-synuclein to form intracellular foci more rapidly than it otherwise would (Fig. 3*C*). These α-synuclein foci were previously shown to occur at sites of stalled vesicles (18). Deletion of Tpo4 had no effect on α-synuclein toxicity, likely due to the redundancy of polyamine transporters in yeast.

Mice Studies Establish a Link Between SAT1 Activity and α-Synuclein Histopathology. To investigate the relationship between SAT1 activity and α-synuclein histopathology in the mammalian brain, we turned to genetically modified mice that express wild-type human α-synuclein and develop histological inclusions (23). Berenil (diminazene aceturate) is a pharmacological agent that reduces SAT1 activity (24), whereas DENSPM (N1, N11-diethylnorspermine) is a polyamine analog that increases SAT1 activity (25). We chronically delivered these agents via osmotic minipumps to the transgenic mouse model. Results showed that, compared with the transgenic mice treated with PBS, neuronal accumulation of α-synuclein in the basal ganglia (Fig. 4*A*) and focused within the substania nigra (Fig. S1) was increased with Berenil ($P = 0.009$) and decreased with DENSPM ($P = 0.043$). Berenil worsened the effects on tyrosine hydroxylase (TH) fibers ($P = 0.033$), whereas DENSPM partially rescued the deficits ($P = 0.022$; Fig. 4*B*). Alterations in the dendritic complexity in the basal ganglia of the α-synuclein transgenic mice were worsened by Berenil ($P = 0.013$) and ameliorated by DENSPM, as detected by MAP2 (Fig. 4*C*). Therefore, overall α-synuclein pathology in these mice was worsened with Berenil and partially rescued with DENSPM. Although comparing drugs to PBS showed no significant effect in nontransgenic mice, general toxicity was associated with the route of administration. Infusion caused

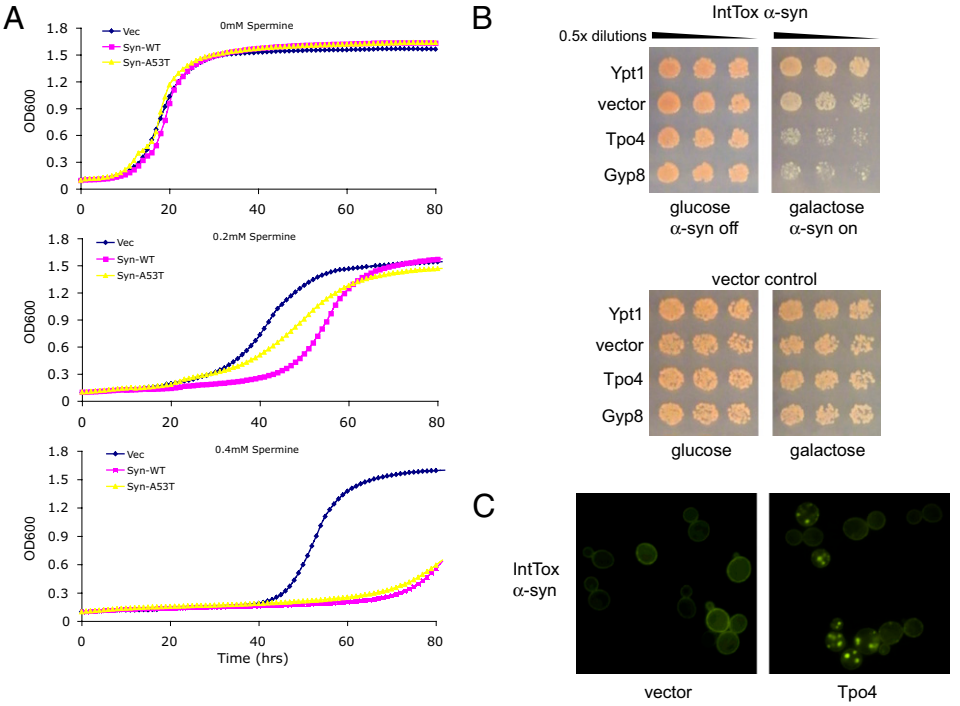

Fig. 3. Yeast studies establish a link between polyamines and α-synuclein. (*A*) Yeast cells integrated with empty vector (Vec), wild-type α-synuclein (Syn-WT), or mutant α-synuclein (Syn-A53T) were grown in YPGal medium supplemented with spermine at concentrations of 0 mM (*Top*), 0.2 mM (*Middle*), and 0.4 mM (*Bottom*). OD_{600} was monitored at 1 h intervals using the Bioscreen system. The growth curves shown are representative of three independent experiments. (*B*) In an unbiased genome-wide yeast screen, Tpo4 was shown to enhance toxicity in cells expressing α-synuclein at a ~40% higher level (IntTox), in comparison with a known toxicity enhancer (Gyp8) and suppressor (Ypt1). (*C*) Tpo4 caused α-synuclein to form intracellular foci more rapidly than it otherwise would in the IntTox strain.

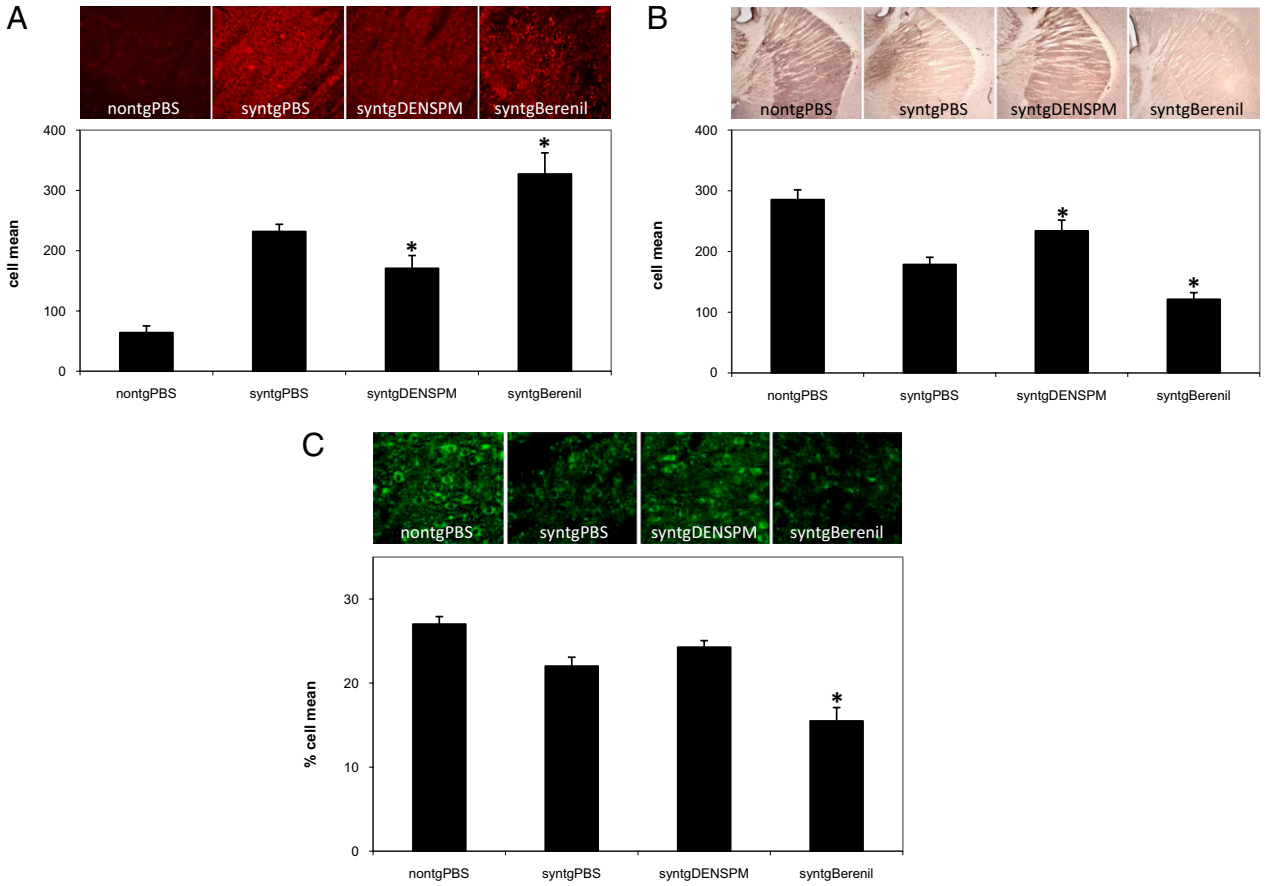

Fig. 4. Mice studies establish a link between SAT1 activity and α-synuclein histopathology. Transgenic mice that express wild-type human α-synuclein and nontransgenic controls (nontg) were treated by intracranial infusion via osmotic pumps with PBS, DENSPM, or Berenil for 6 wk. Results for immunoreactivity within the basal ganglia are shown. (*A*) Mean α-synuclein cell-pixel intensity (cell mean) in the caudoputamen was increased with Berenil (**P* = 0.009) and decreased with DENSPM (**P* = 0.043) in comparison with transgenic α-synuclein mice treated with PBS (syntgPBS). (*B*) Tyrosine hydroxylase (TH) fibers were decreased with Berenil treatment (**P* = 0.033), and increased with DENSPM (**P* = 0.022), compared with syntgPBS, as shown by the cell mean (TH corrected optical density in the caudoputamen). (*C*) Berenil caused a decrease in MAP2 (**P* = 0.013), compared with syntgPBS, whereas DENSPM rescued the transgenic α-synuclein effects. Percent cell mean represents the percentage of the neuropil covered by MAP2 immunoreactive dendrites in the caudoputamen.

death before the termination of the experiment in some of the control and pharmacologically treated mice.

Genetic Studies Identify a PD-Associated Variation in the SAT1 Gene. To investigate a genetic link between SAT1 and PD, all exons and adjacent exon/intron boundaries of the SAT1 gene were sequenced in a total of 92 PD patients. We identified a variant, c.786_788delTGT (NM_002970), in the 3′UTR of the SAT1 gene in two PD patients (Fig. 5). One patient was heterozygous and one hemizygous for the c.786_788delTGT variant. To evaluate the frequency of the 3′UTR variant, we extended the analysis to genotyping of additional patients and controls enrolled in the genetic epidemiology of PD, GEPD (total: $n = 797$ subjects; patients: $n = 389$; and controls: $n = 408$). Overall, a total of four PD patients were identified that carried the c.786_788delTGT variant, including three heterozygotes and one hemizygote. The c.786_788delTGT variant was absent in all 816 control chromosomes ($n = 408$ controls). The mean age of the four PD patients carrying the c.786_788delTGT variant was 63.3 (range 51–72), the mean age at onset was 54 y (range 38–68, with two having onset <50), and mean duration of PD was 9.25 y (SD 7.5). There were three women and one man, and three Caucasian and one "Other" ethnicity. None reported a family history of PD in a first-degree relative. Three of the four had tremor at rest as a first symptom, and all were levodopa responsive. None of the four were demented at the time of evaluation. None of the cases carried mutations in Parkin, LRRK2, or DJ1. Lymphoblasts were available in only one PD case carrying the SAT1 c.786_788delTGT variant of the gene, and four noncarrier male patients. In this limited sample, a reliable effect of the variant on SAT1 mRNA expression, degradation, or stability could not be documented (for more experimental detail, see *SI Text*).

Discussion

To date, uncovering pathogenic molecular pathways associated with neurodegeneration has relied primarily on biochemical analysis of protein aggregates or on linkage analysis to isolate genetic mutations. These two approaches have been important in clarifying the molecular biology of neurodegeneration (2), and have been successful in identifying pathogenic molecules underlying rare, monogenic forms of disease. The introduction of gene expression profiling techniques has allowed the focus of molecular discovery to shift from aggregates and genes to brain cells themselves. Reflecting an interaction among multiple genetic and epigenetic factors, expression profiles of affected cells are, in principle, well suited for uncovering pathogenic pathways underlying complex disorders of the brain (4). When applied to neurodegenerative diseases, however, gene expression studies present a number of analytic challenges, including poor signal-to-noise and high false-positivity (4). Furthermore, observed expression differences are only correlative and cannot, by themselves, establish a pathogenic link to disease.

fMRI-Guided Microarray. In attempting to address the analytic challenges of microarray, we were guided by our previous studies that used microarray to identify retromer trafficking defects as pathogenic in late-onset Alzheimer's disease (AD) (26, 27). First, we needed to identify neighboring regions within the same brain

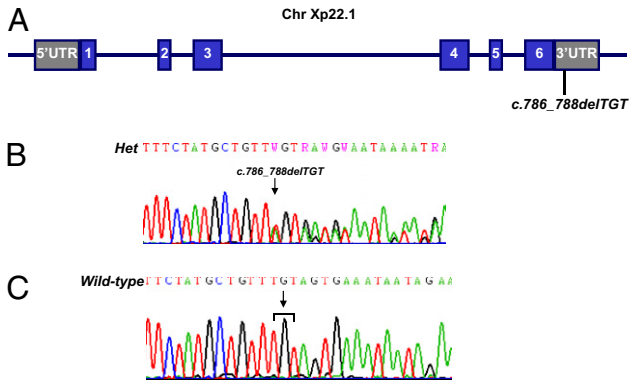

Fig. 5. Genetic studies in human patients identify a PD-associated variance in SAT1. (*A*) Schematic of the SAT1 gene and the location of the deletion within the 3′UTR of SAT1. (*B*) Sequence chromatograms showing a PD patient heterozygous for the c.786_788delTGT variant, and (*C*) a wild-type subject.

structure, differentially affected and resistant to PD. Deciding to focus on the brainstem, a structure purposed to be affected early on in the disease course, we exploited the high-resolution capabilities of basal CBV mapping with fMRI. Previous studies have established the utility of CBV fMRI in mapping brain function (28) and have shown that basal CBV is tightly correlated with disease-associated metabolic dysfunction (29). Most importantly, compared with other hemodynamic variables used in fMRI—i.e., cerebral blood flow or deoxyhemoglobin—CBV generates functional maps with the highest spatial resolution (9).

Just as we have used CBV fMRI to identify hippocampal subregions differentially affected and resistant to AD, we reasoned that this high-submillimeter resolution might be used to map dysfunction in small regions of the brainstem. Indeed, our first fMRI study identified the DMVN as a brainstem region differentially affected by PD, and the ION as a neighboring region relatively resistant to the disease. Future large-scale imaging studies, in which brainstem CBV maps are generated in a larger number of PD patients across different stages of the disease, are required to determine whether observed brainstem dysfunction correlates with signs and symptoms of the disease, whether it antedates dysfunction in other brain regions, and whether it can be used for diagnostic purposes.

Guided by our fMRI results, we harvested the DMNV and ION in postmortem brains with and without PD, and by profiling expression levels in each individual tissue sample we were able to perform a "double subtraction" factorial ANOVA. As previously described, when applied to a microarray dataset, this statistical design improves the odds that the isolated molecules are linked to the disease (4, 5).

Validating the Microarray Finding. Although the list of molecules that emerged from the factorial ANOVA are likely linked to PD, this analysis cannot identify which molecular findings play a causal role in disease pathogenesis. As in all neurodegeneration, the disease process in PD exists many years before the patient's death, and it is impossible to know whether a postmortem finding reflects an upstream defect that affects α-synuclein toxicity, or a downstream effect reflecting protracted neuronal dysfunction. Thus, a range of additional studies are required to interpret the mechanistic and causal role of any microarray finding identified in postmortem samples (4). For example, in our previous studies, imaging-guided microarray applied to AD identified deficiencies in the retromer trafficking pathway (27). However, only by systematically manipulating retromer-related molecules—in cell culture (27), animal models (26)—and by linking genetic variance to the disease in human patients (30), was this trafficking pathway pathogenically linked to AD (31).

Among the transcripts identified in the microarray study, we decided to focus our attention on the observed decrease in SAT1 expression. SAT1 is the rate-limiting enzyme in polyamine catabolism, and a reduction in SAT1 leads to an increase in higher-order polyamines—in particular, spermidine and spermine (24, 32). A previous study showed that PD patients have elevated levels of spermidine and spermine in red blood cells (13), which do not themselves produce polyamines. Another study showed that in an in vitro system, exogenously added spermidine and spermine accelerate the aggregation of α-synuclein (12). Furthermore, previous studies have shown that SAT1 is expressed in numerous brain regions implicated in PD, including the substantia nigra pars compacta (33).

Whether polyamines can modify the cellular toxicity of α-synuclein in vivo was unknown. To address this issue, we turned to a yeast model of PD and showed in an unbiased screen that Tpo4, responsible for polyamine transport in *S. cerevisiae*, and exogenous spermine accelerated the toxicity of yeast expressing human α-synuclein. Importantly, because we are interested in sporadic PD, in which nonmutated forms of α-synuclein play a mechanistic role, acceleration of the phenotype was found in yeast expressing wild-type α-synuclein.

The next question was whether SAT1 activity can modify α-synuclein histopathology in the mammalian brain. To address this question, we turned to a transgenic mouse model of PD that expressed wild-type human α-synuclein, and treated them with pharmacological agents, Berenil and DENSPM. Berenil (diminazene aceturate) has been shown to inhibit polyamine metabolism by reducing SAT1 activity via competitive inhibition of the enzyme (24). Berenil was favored above other SAT1 inhibitors due to its selectivity for effecting SAT1 alone, and no other enzymes involved in polyamine metabolism (34). DENSPM (N1, N11-diethylnorspermine) is a polyamine analog and the most potent known inducer of SAT1 activity. A number of studies have demonstrated DENSPM's ability to down-regulate polyamine biosynthetic enzyme activities and suppress transport of polyamines, as well as its potent up-regulation of SAT1, resulting in depletion of intracellular polyamine pools (35, 36). Using these pharmacological agents that mediate SAT1 activity, findings showed that Berenil worsened the PD phenotype, whereas DENSPM partially improved the PD phenotype in these mice.

Finally, we decided to sequence SAT1 in human patients, even though a genetic variant in this gene was not necessarily assumed. In fact, as a complex disorder, we believe that polyamine abnormalities observed in PD are more likely to reflect a complex interaction between genes, epigenetics, and the environment rather than defects in the SAT1 gene itself. However, because any genetic finding in human patients would strengthen a pathogenic link, we reasoned that it was worth exploring this issue. Remarkably, a unique variant, c.786_788delTGT, in the SAT1 gene was indeed found. It is important to note that this variant is rare, occurring in less than 1% of the patients examined, but was exclusive to patients and absent in all 816 of the control chromosomes genotyped. Additionally, based on a small number of samples, we have not yet determined whether this genetic variant affects expression levels or otherwise affects the function of SAT1. Beyond the scope of the current body of work, future genetic studies genotyping a larger number of cases and controls are required to determine the exact frequency of c.786_788delTGT, and future molecular studies will determine whether and how this variant affects the enzymatic function of SAT1. Despite these unanswered questions, the surprising disease-associated mutation identified in SAT1 does, we believe, strengthen the link between the polyamine pathway and PD.

Conclusions

Although spanning a broad range, the studies presented in patients, yeast and mouse models, are unified in their attempt to confirm the pathogenicity of the microarray finding. Taken as a whole, these complementary studies suggest that defects in the polyamine pathway play a role in PD pathogenesis, and the findings have immediate clinical implications. First, because polyamines can be measured in cerebral spinal fluid and blood, serological analysis might be able to detect polyamine abnormalities and can be used for early detection of PD and for monitoring therapeutic interventions. Second, and perhaps more importantly, a number of pharmacological agents have already been developed that enhance the function of SAT1 and polyamine metabolism (37). Based on our present findings, we have begun exploring whether any of these agents cross the blood–brain barrier, and if so, plan on initiating drug studies to de-

termine whether reductions of brain polyamine levels ameliorate this common and undertreated disease.

Materials and Methods

Brain Imaging Studies. ***Subjects, data acquisition, and processing.*** See *SI Text*.
Data analysis. **Unbiased pixel-based analysis.** All CBV maps of the target slice were spatially filtered and coregistered; on a pixel-by-pixel basis, a *t*-test was used comparing the grouped PD images to the grouped control images. The yielded *z*-score was then colorwashed onto the standard anatomical image for visual inspection (Fig. 1*B*).

Hypothesis-driven ROI-based analysis. Performed as previously described (38); for details, see *SI Text*.

Postmortem Studies. ***Gene expression profiling.*** Total RNA was extracted from each of the 22 tissue samples with TRIzol reagent (Invitrogen) and purified with RNeasy mini columns (Qiagen). All subsequent steps followed Affymetrix's Eukaryotic Target Preparation Protocol found in the GeneChip Expression Analysis Technical Manual (for details, see *SI Text*).
Western blot analysis. A new set of five PD and five control brain samples were obtained from the New York Brain Bank at Columbia University, following the criteria described in *SI Text*. Within each brain, the DMNV and ION were identified and sectioned using strict anatomical criteria. Tissue samples were prepared as previously described (27); for details, see *SI Text*.
Immunohistochemistry. Axial blocks of human medulla oblongata were frozen-sectioned using a Microm cryostat at 8-μm thickness as previously described (27); for details, see *SI Text*.

Yeast Studies. ***Yeast strains, media, and growth-rate assays.*** See *SI Text*.
Yeast screen. Tpo4 was identified in an unbiased genome-wide screen investigating modifiers of α-synuclein toxicity (21); see *SI Text* for details.
α-Synuclein growth with Tpo4. α-Synuclein strains and control strains were grown overnight to saturation in glucose-containing media. Cultures were normalized for their OD and serially diluted fivefold before spotting onto yeast media plates containing either glucose or galactose.
α-Synuclein microscopy. Cells were grown overnight in glucose-containing media. Culture densities were normalized, washed with water, and induced for 6 h in galactose. Cells were fixed [4% formaldehyde, 50 mM KPi (pH 6.5), 1 mM MgCl2] for 1 h on ice, washed twice with PBS, and imaged.

Transgenic Mice Studies. ***α-Synuclein transgenic mice and infusion.*** For this study, heterozygous transgenic (tg) mice (line 61) expressing wild-type human α-synuclein under the regulatory control of the mThy1 promoter were used (23). For details on these mice and the infusions, which were described previously (39), see *SI Text*.
Immunohistochemical analysis of α-synuclein accumulation and neurodegeneration. Immunohistochemistry was performed as described previously; for details, see *SI Text*.

Genetic Studies. Details on patient population can be found in *SI Text*.
Sequencing and genotyping. PCR and amplification of all exons and exon/intron boundaries of the SAT1 gene were performed. The PCR and sequencing primers used for amplification of SAT1 are available upon request. Cycle sequencing in forward and reverse directions was performed on purified PCR products and run on an ABI 3700 genetic analyzer (Applied Biosystems). Sequence chromatograms were viewed and genotypes determined using Sequencher (Genecodes).
Statistical analysis. See *SI Text*.
Protein, mRNA levels, and stability of splice variants. See *SI Text*.

ACKNOWLEDGMENTS. We thank those who willingly participated in the studies presented herein. This work was supported in part by awards from the McKnight Endowment for Neuroscience (to S.A.S., D.R., and G.A.P.), National Institutes of Health Grants AG18440, AG022074 (to E.M.), NS038372 (to S.L.), UL1 RR024156 (to K.M.), and NS36630, and the Parkinson's Disease Foundation (to K.M. and L.N.C.). M.L.G. is supported by a National Institutes of Health postdoctoral fellowship.

1. Hardy J, Cai H, Cookson MR, Gwinn-Hardy K, Singleton A (2006) Genetics of Parkinson's disease and parkinsonism. *Ann Neurol* 60:389–398.
2. Litvan I, et al. (2007) The etiopathogenesis of Parkinson disease and suggestions for future research. Part I. *J Neuropathol Exp Neurol* 66:251–257.
3. Coppola G, Geschwind DH (2006) Technology insight: Querying the genome with microarrays—progress and hope for neurological disease. *Nat Clin Pract Neurol* 2: 147–158.
4. Lewandowski NM, Small SA (2005) Brain microarray: Finding needles in molecular haystacks. *J Neurosci* 25:10341–10346.
5. Kerr MK, Martin M, Churchill GA (2000) Analysis of variance for gene expression microarray data. *J Comput Biol* 7:819–837.
6. Braak H, et al. (2003) Staging of brain pathology related to sporadic Parkinson's disease. *Neurobiol Aging* 24:197–211.
7. Simuni T, Sethi K (2008) Nonmotor manifestations of Parkinson's disease. *Ann Neurol* 64 (Suppl 2):S65–S80.
8. Pfeiffer RF (2003) Gastrointestinal dysfunction in Parkinson's disease. *Lancet Neurol* 2: 107–116.
9. Lin W, Celik A, Paczynski RP (1999) Regional cerebral blood volume: A comparison of the dynamic imaging and the steady state methods. *J Magn Reson Imaging* 9:44–52.
10. Moreno H, et al. (2007) Imaging the Abeta-related neurotoxicity of Alzheimer disease. *Arch Neurol* 64:1467–1477.
11. Marton LJ, Pegg AE (1995) Polyamines as targets for therapeutic intervention. *Annu Rev Pharmacol Toxicol* 35:55–91.
12. Antony T, et al. (2003) Cellular polyamines promote the aggregation of alpha-synuclein. *J Biol Chem* 278:3235–3240.
13. Gomes-Trolin C, Nygren I, Aquilonius SM, Askmark H (2002) Increased red blood cell polyamines in ALS and Parkinson's disease. *Exp Neurol* 177:515–520.
14. Chen G, et al. (2002) Discordant protein and mRNA expression in lung adenocarcinomas. *Mol Cell Proteomics* 1:304–313.
15. Grabenauer M, et al. (2008) Spermine binding to Parkinson's protein α-synuclein and its disease-related A30P and A53T mutants. *J Phys Chem B* 112:11147–11154.
16. Cooper AA, et al. (2006) Alpha-synuclein blocks ER-Golgi traffic and Rab1 rescues neuron loss in Parkinson's models. *Science* 313:324–328.
17. Outeiro TF, Lindquist S (2003) Yeast cells provide insight into alpha-synuclein biology and pathobiology. *Science* 302:1772–1775.
18. Gitler AD, et al. (2008) The Parkinson's disease protein α-synuclein disrupts cellular Rab homeostasis. *Proc Natl Acad Sci USA* 105:145–150.
19. Conway KA, Harper JD, Lansbury PT (1998) Accelerated in vitro fibril formation by a mutant alpha-synuclein linked to early-onset Parkinson disease. *Nat Med* 4:1318–1320.
20. Polymeropoulos MH, et al. (1997) Mutation in the alpha-synuclein gene identified in families with Parkinson's disease. *Science* 276:2045–2047.
21. Yeger-Lotem E, et al. (2009) Bridging high-throughput genetic and transcriptional data reveals cellular responses to alpha-synuclein toxicity. *Nat Genet* 41:316–323.
22. Tomitori H, et al. (2001) Multiple polyamine transport systems on the vacuolar membrane in yeast. *Biochem J* 353:681–688.
23. Rockenstein E, et al. (2002) Differential neuropathological alterations in transgenic mice expressing alpha-synuclein from the platelet-derived growth factor and Thy-1 promoters. *J Neurosci Res* 68:568–578.
24. Libby PR, Porter CW (1992) Inhibition of enzymes of polyamine back-conversion by pentamidine and berenil. *Biochem Pharmacol* 44:830–832.
25. Thomas T, Thomas TJ (2001) Polyamines in cell growth and cell death: molecular mechanisms and therapeutic applications. *Cell Mol Life Sci* 58:244–258.
26. Muhammad A, et al. (2008) Retromer deficiency observed in Alzheimer's disease causes hippocampal dysfunction, neurodegeneration, and Abeta accumulation. *Proc Natl Acad Sci USA* 105:7327–7332.
27. Small SA, et al. (2005) Model-guided microarray implicates the retromer complex in Alzheimer's disease. *Ann Neurol* 58:909–919.
28. Belliveau JW, et al. (1991) Functional mapping of the human visual cortex by magnetic resonance imaging. *Science* 254:716–719.
29. González RG, et al. (1995) Functional MR in the evaluation of dementia: correlation of abnormal dynamic cerebral blood volume measurements with changes in cerebral metabolism on positron emission tomography with fludeoxyglucose F 18. *AJNR Am J Neuroradiol* 16:1763–1770.
30. Rogaeva E, et al. (2007) The neuronal sortilin-related receptor SORL1 is genetically associated with Alzheimer disease. *Nat Genet* 39:168–177.
31. Small SA (2008) Retromer sorting: A pathogenic pathway in late-onset Alzheimer disease. *Arch Neurol* 65:323–328.
32. Niiranen K, et al. (2006) Mice with targeted disruption of spermidine/spermine N1-acetyltransferase gene maintain nearly normal tissue polyamine homeostasis but show signs of insulin resistance upon aging. *J Cell Mol Med* 10:933–945.
33. Zoli M, Pedrazzi P, Agnati LF (1996) Regional and cellular distribution of spermidine/spermine N1-acetyltransferase (SSAT) mRNA in the rat central nervous system. *Neurosci Lett* 207:13–16.
34. Wallace HM, Fraser AV (2004) Inhibitors of polyamine metabolism: Review article. *Amino Acids* 26:353–365.
35. Porter CW, Ganis B, Libby PR, Bergeron RJ (1991) Correlations between polyamine analogue-induced increases in spermidine/spermine N1-acetyltransferase activity, polyamine pool depletion, and growth inhibition in human melanoma cell lines. *Cancer Res* 51:3715–3720.
36. Casero RA, Jr, et al. (1989) Differential induction of spermidine/spermine N1-acetyltransferase in human lung cancer cells by the bis(ethyl)polyamine analogues. *Cancer Res* 49:3829–3833.
37. Gerner EW, Meyskens FL, Jr (2004) Polyamines and cancer: Old molecules, new understanding. *Nat Rev Cancer* 4:781–792.
38. Schobel SA, et al. (2009) Differential targeting of the CA1 subfield of the hippocampal formation by schizophrenia and related psychotic disorders. *Arch Gen Psychiatry* 66:938–946.
39. Veinbergs I, et al. (2001) Role of apolipoprotein E receptors in regulating the differential in vivo neurotrophic effects of apolipoprotein E. *Exp Neurol* 170:15–26.